Comparative study on Radio Refractivity Gradient in the troposphere using Chaotic Quantifiers

J.S. Ojo, A.O. Adelakun *, O.V. Edward

Department of Physics, Federal University of Technology, Akure, Ondo state, Nigeria

ARTICLE INFO

ABSTRACT

Complexity and nonlinear trend in the internal activities of the troposphere has been a great factor affecting the transmission and receiving of good quality of signals globally. In lieu of this, prediction of chaos and positive refractivity gradients for line-of-sight microwave radio paths is necessary for designing radio systems. Complexity in the troposphere due to changes in meteorological parameters can lead to the strong negative gradient (or super-refraction) which afterward lead to interference between terrestrial links and satellite earth stations. In this paper, a comparative study on the degree of complexity of Radio Refractivity Gradient (RRG) using Chaotic Quantifiers (CQ) such as Phase Plot Reconstruction (PPR), Average Mutual Information (AMI), False Nearest Neighbor (FNN), Lyapunov Exponent (LE), Tsallis Entropy (TS) and Recurrence Plot (RP) are discussed extensively. The RRG data (2011-2012) used in this work were obtained for 0 m to 100 m, from the archives of Tropospheric Data Acquisition Network (TRODAN) from five different stations namely; Akure (*Geo*. $7.299°N, 5.147°E$), Enugu (*Geo*. $6.46°N, 7.55°E$), Jos (*Geo*. $9.90°N, 8.86°E$), Minna (*Geo*. $9.58°N, 6.55°E$) and Sokoto (*Geo*. $13.01°N, 5.25°E$). The chaotic quantifiers are used to investigate the degree of complexity in the 30 minutes interval atmospheric data from the selected locations which is specified into rainy, dry and transition season months. The parallel and short diagonal lines observed depicts the evidence of chaos. However, the observed result shows that the RRG is higher during the rainy season than the dry season. In other words, the information is valid for the proposed data analysis, since the LE is actually directly proportional to the TE. Also, the results further show that the rainy season months exhibit higher chaoticity than the dry season months, which is equivalent to high radio refractivity gradient observed across the selected stations.

1. Introduction

Global radio link fading has been an issue in recent years in microwave communication services [1]. In Nigeria, different activities emerging from meteorological parameters and hydrometeors has been some of the major factors affecting radio propagation. Atmospheric meteorological parameters such as relative humidity, temperature, pressure, and water vapor density increase the complexity of the troposphere and significantly has a great influence on microwave propagation above 30 MHz. They combine in many ways to affect radio wave propagation and the radio refractivity gradient in the tropics, particularly, in the coastline [1, 2]. It is worth noting that the refractivity of the atmosphere will not only vary as the height changes but will also affect radio signals. The choice of the troposphere in this paper lies on the fact that the region between 0 m and 100 m has the highest concentration of water vapor, and makes it difficult for propagating the radio-link net-

work. The prevalence of sea and land breezes which play a major role in the development and intensification of weather events also accounts for the high concentration of water vapor in the coastal cities [3, 4, 5, 6]. Refractivity gradient in 1 km interval above ground are important for the estimation of super–refraction and ducting phenomena, and their effects on radar observations and Very high frequency (VHF) the field strength at points beyond the horizon cannot be undermined [7]. It is a well-known fact that refractivity gradients can be determined either by the direct method using refractometers or indirectly using a fixed measuring methods such as TV tower, radiosonde measurement, remote sensing techniques, statistical and deterministic model [8]. In this paper, there is still the need to further extend the research to different locations and compare the complexity and the chaotic trends vividly. This paper, therefore, assesses the complexity in the dynamical activities of the radio refractivity gradient in the troposphere using chaotic quantifiers. Aside from time series and phase plot reconstruction, the

---

paper also employed Average Mutual Information (AMI), False Nearest Neighbor (FNN), Lyapunov Exponent (LE), Tsallis Entropy (TE) and Recurrence Plot (RP) to analyze radio refractivity gradient between 2011 and 2012 using Atmospheric data. Unlike previous research, where the focus is mainly on a single station "Akure" in Nigeria using different heights [8, 9], while the present research actually covers selected stations across Nigeria with emphasis on rainy season, dry season and transition periods. The onset of the dry season, October and November, and the onset of the rainy season, March and April, serves as the rain-harmattan transition phase and it was chosen for consideration. The seasonal rain-harmattan transition phase, is dry and characterized by dust-laden north-easterly wind, which pushes southward towards the coastal cities of West Africa due to the West African Monsoon (WAM) [10, 11, 12] as part of the global circulation system [13, 14] in response to the Madden-Julian Oscillation (MJO) [15]. Also, the reports on the dry and rainy season months are due to the polarizability of both non-polar (chiefly, nitrogen and oxygen) and polar (mainly, water vapor) molecules, respectively [1].

2. Theory

2.1. Radio Refractivity Gradient (RRG)

Multipath fading occurs as a result of signal encountering an obstacle leading to different paths before getting to the target. This problem leads to interference along the propagation of signals in the troposphere. The fading due to multipath may also arise as a result of variation in the refractive index in the atmosphere especially at the horizontal layers with different refractivity. The result of the large variation of the refractive index in the atmosphere is needed to determine the radio refractivity that affects radio wave along with the terrestrial radio links. The information is also vital for planning and design acceptable radio links for satellite networks, radar among others.

Nigeria as a tropical country, witness both rainy season and dry season within a year which is usually accomplished with transition periods (i.e. the on-set and off-set of rainy-harmattan period). With problem at hand, fading or failure in the network needs to be investigated using CQs are expected to give better information on the internal activities in the troposphere. However, the radiowave propagation is usually influenced by changes in the refractive index, n, of air in the troposphere. The refractive index, n, can be expressed in terms of radio refractivity, N as [1, 17]:

$$n = 1 + N \times 10^6 \tag{1}$$

The multiplication factor in equation (1) was used because the refractive index, n, for air deviates from unity by at most a few parts per ten thousand [16]. Radio refractivity, (N), which is the sum of the dry and wet parametric values, can be expressed as [17]:

$$N = 77.6\frac{P}{T^2} + 3.73 \times 10^5 \frac{e}{T^2} \tag{2}$$

The Clausius-Clapeyron relationship between water vapor pressure, e (hPa), saturation vapor pressure, e_s (hPa) and relative humidity, H (%), can, therefore, be deduced from equation (2) as:

$$e = \frac{H}{100} e_s \tag{3}$$

where

$$e_s = a \exp[\frac{bt}{t+c}] \tag{4}$$

The parameters in (4) are derived as $a = 6.1121$, $b = 17.502$, $c = 240.97$. T is the atmospheric temperature in K, dry atmospheric pressure P in hPa, and t is the temperature in °C. Therefore, RRG in N-units/km, can be expressed as:

$$RRG = \frac{dN}{dh} \tag{5}$$

$$RRG = -7.32 \exp(0.005577 \times N_s)(N - units/km) \tag{6}$$

In Eqn. (5), N_s are the values of radio refractivity at the ground surface level and the RRG-value determines the anomalous behavior of microwave propagation in the troposphere. The influence of RRG, especially at the lower part of the atmosphere, leads to propagation effects like super-refraction, sub-refraction, or ducting [18].

2.2. Time series and Phase Plot Reconstruction (PPR)

In nonlinear science, the physical appearance of a dynamic ensemble can be represented by the nonlinear time series. However, the series may not actually display the internal display of the dynamics which implies that it may not reveal the whole process going on in the system. A natural system like the troposphere is a very good example that can simply be described as an unpredictable dynamical ensemble. Due to the movement of different micro-ensemble assemble to form macro-ensemble such as the troposphere, the expectation of the dynamic state will be complex and not in any way reliable for predicting the radio path in the area of communication. For example, in this work, the time series for the radio refractivity gradient was categorized into rainy season months such as June, July, August, and September, while the dry season anomalies were captured in December, January and February. Also, the transition periods such as March, April, October, and November were discussed.

The case of phase space reconstruction was based on the embedding theorem given as:

$$Y_n = (s_n - (m - 1)\tau, s_n - (m - 2)\tau, ..., s_n), \tag{7}$$

where Y_n is the phase space vectors, s_n is the time series which is a sequence of scalar measurement of the same quantity taken as a series at different portions in time t for a given time interval (δt). The three-dimensional phase space reconstruction reported in this work, depends on the proper choice of the determinant parameters, the embedding dimension (m) and the delay time (τ), which are more important in phase space reconstruction [19, 20].

2.3. Average Mutual information (AMI) and False Nearest Neighbor (FNN)

To obtain coordinates for time-delayed phase space embedding that is independent as possible, there is the need to compute for a time series and a time-shifted version of the same time series called auto mutual information i.e. autocorrelation function. The expression for the AMI is given by:

$$I(x(t), x(t + \tau)) = \sum_{i,j} p_{ij}(\tau) log(\frac{p_{ij}(\tau)}{p_i p_j}). \tag{8}$$

Here, p_j is the probability that $x(t)$ is in bin i of the histogram constructed from the data points in x, and $p_{ij}(\tau)$ is the probability that $x(t)$ is in bin i and $x(t + \tau)$ is in bin j. It is worth noting that only joint probability $p_{ij}(\tau)$ that depend on time delay (τ). Also, taking into consideration that AMI likewise depends on the way the histogram width is constructed.

However, the method of FNN measures the percentage of closeness, in terms of Euclidean distances, of neighboring points of the trajectory in a given dimensional space, and compares it with the next dimensional space (i.e. reduce the fraction of FNN to the minimal). If the ratio of these distances is greater than a predefined threshold due to a change in dimension, the neighbors of the trajectory are considered as false neighbors. The value of the predefined threshold should be sufficiently large so that it will allow the exponential divergence of the chaotic signal. In practice, the value of the threshold is chosen between 10 to 50 [21].

The idea of underlying the estimation of embedding dimension using a false nearest neighbor is suggested as if two points are close to each other for one-dimensional time series i.e. adjacent, then they are neighbors [22]. With this information, the distance between the neighbors can be measured by finding the difference in their magnitude. For example, assume we embed the time series once in two dimensions using time delay (τ), then we examine the distance between the neighbors by using the corresponding coordinates of the same data points. If the embedding changes appreciably towards the distance between the neighbors, then they are dubbed false neighbors which imply that the data can still be embedded further. But, if there are no appreciable changes, then it is dubbed true neighbors and leaves the shape of the attractor unchanged.

The false nearest neighbor can be computed using the formula proposed by Kennel et al. [22]. Considering the D-dimensional phase space with rth nearest neighbor of a coordinate vector $y(t)$ represented by $y^{(}r)(t)$, then the square of the Euclidean distance (R_D) between time series $y(t)$ and the rth nearest neighbor is given as:

$$R_D^2(t,r) = \sum_{k=0}^{D-1}[x(t+k\tau) - x^{(r)}(t+k\tau)]^2 \tag{9}$$

With the addition of new coordinate to time series ($y^{(r)}t$), then the D-dimensional phase space can be shifted into (D+1)-dimensional phase-space by time-delayed embedding. Hence, Eq. (8) can be re-written as:

$$R_{D+1}^2(t,r) = R_D^2(t,r) + [x(t+D\tau) - x^{(r)}(t+D\tau)]^2 \tag{10}$$

From Eq. (8) and Eq. (9), the distance (R_D) between the Euclidean y(t) and the rth nearest neighbor can also be expressed in term of tolerance threshold as:

$$[\frac{R_{D+1}^2(t,r) - R_{D(t,r)}^2}{R_{D(t,r)}^2}]^{1/2} = \frac{|x(t+D\tau) - x^{(r)}(t+D\tau)|}{R_D^2(t,r)} > R_{tol} \tag{11}$$

2.4. Lyapunov exponents and Tsallis entropy

The LE is one of the mathematical tools in investigating the state of any dynamical system. When the LE is positive, then the system is chaotic, otherwise, periodic if the LE is negative. This tool indicates divergence of trajectory or expansion of volume alternatively for positive LE, while a negative value of LE indicates convergence or contraction of volume. The maximum or Largest LE (λ_1) [23], can be expressed as:

$$\lambda_1 = \lim_{r \to inf} \frac{1}{t} log \frac{\triangle x(t)}{x(0)} \tag{12}$$

$$\lambda_1 = \lim_{r \to inf} \frac{1}{t} \sum_{i-1}^{t} log \frac{\triangle x(t_i)}{\triangle x(t_i-1)} \tag{13}$$

TE, on the other hand, can be used to describe the dynamic complexity of any natural system such as internal activities in the troposphere. For example, in the area of information theory, TE was inspired by the probabilistic description of multi-fractal geometries. The statistical tool then characterizes the amount of information stored by measuring the probability distribution or uncertainty of the system internal activities [24, 25, 26, 27]. The TE in term of index q can then be expressed as:

$$S_q = k\frac{1}{q-1}(1 - \sum_{i=1}^{W} p_i^q) \tag{14}$$

where W is the total number, k is Boltzmann's constant, p_i is the probability associated with the microscopic configuration. The value of q is real which indicate the measure of the non-extensivity of a system i.e. as q tends to 1, the system becomes standard extensive Boltzmann-Gibbs statistics. In addition, the entropy index q also characterized the degree of nonadditivity reflected in the pseudo-additive rule:

$$S_q(A + B) = S_q(A) + S_q(B) + (1-q)S_q(A)S_q(B) \tag{15}$$

In addition, non-extensive case of TE was also discovered to vary directly as Kolmogorov-Sinai produced from LE for logistic maps and dynamical systems, in the threshold of chaos where $\lambda = 0$, when $q = 1$ in a chaotic region. It is worthy to note that index q is not actually used to quantify the complexity but rather to measure the degree of non-extensive of the system. If $q < 1$, then the system is sub-extensive (or sub-additive) and when $q > 1$, the system is super-extensive (or super-additive). In essence, if the subsystem has special theory probability correlation, extensively is not valid for Boltzmann-Gibbs entropy. Such systems are generally referred to as non-extensive systems [28, 29, 30]. However, when the TE (S_q) values is lower, then the region with lower complexity is revealed.

The investigation of dynamic complexity using TE has been extended to the magnetosphere [29, 30] and ionosphere [21], therefore, there is the need for further investigation on the complexity of RRG of the troposphere. The fact is that the chaotic response and weak chaos of TE have been investigated due to its non-extensive nature in the troposphere [31, 32]. Similarly, the report on varnishing largest LE has been discussed extensively and its relationship to TE has been justified [33, 34]. Further research by Coraddu et al. [35], suggests the exponential behavior for a chaotic regime where a large class of generalized exponential shows the same behavior.

$$q \to 1 \tag{16}$$

$$\lim_{q \to 1} exp(\lambda_q t) = exp(\lambda t) \tag{17}$$

The work of Anastasiadis et al. [29] explored different choice of index q for a dynamical system, suggesting $\lambda < 0$ for periodic regime, $\lambda = 0$ edge of chaos and $\lambda > 0$ for a chaotic region. This implies that the degree of complexity in the troposphere depend on the choice of index q.

2.5. Recurrence Plot (RP)

This is based on the RP discovery by Eckmann et al. [36] which basically focused on time-dependent of the dynamic systems. The recurrence plot visualized the state-space dynamics which has been pictured on phase space reconstruction. The recurrence plot can be expressed as:

$$R_{ij} = \Theta[\epsilon_i - \|\overline{x}_i - \overline{x}_j\|], \tag{18}$$

$$i, j = 1, ..., N \tag{19}$$

where R_{ij} is the recurrence matrix, ϵ is a predefined threshold characterizing the distance between two neighboring points, $\|.\|$ is a Euclidean norm, N is the number of the considered state x_i. x_i and x_j are the phase space point at times i and j, respectively, while Θ is the Heaviside function. The qualitative picture or feature of a recurrence plot has been defined by Eckmann et al. [36] as typology while Marwin [37] as texture. However, a recurrence point state in phase space at the time i at different time j is denoted within a two-dimensional squared matrix, in which "black" dot represents one while white dot signifies zero. According to Thiel et al. [38], the "black" dot implies the returning of the system to a neighborhood of the corresponding point in phase space.

3. Methodology

The study area for this research covers five different tropical zones located in Nigeria namely; Akure (*Geo.* 7.299°N, 5.147°E), Enugu (*Geo.* 6.46°N, 7.55°E), Jos (*Geo.* 9.90°N, 8.86°E), Minna (*Geo.* 9.58°N, 6.55°E) and Sokoto (*Geo.* 13.01°N, 5.25°E). The research locations lie between Lat. 3° and 15° and Long. 3° and 14°. The data used in this research work were obtained from the archives of Tropospheric Data Acquisition Network (TRODAN) domiciled with the Centre for Atmospheric Research, National Space Research, and Development Agency, Anyigba, Kogi State, Nigeria. The RRG data for 0 to 100 m were obtained and used. In addition, the data for the five selected locations were recorded
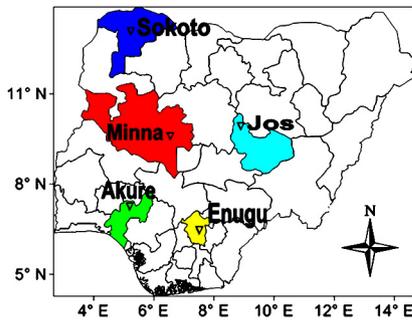
Fig. 1. Typical Map of Nigeria, showing the Location of the Study areas.

in 30 minutes interval from January 1, 2011 to December 31, 2012. Finally, the data recorded cover 24 hours each day from 00:00 hours to 23:00 hours local time at 30 minutes interval involving the dry, transition and rainy season months of the year. The rainy season months are between the months of May and September; the transition months (March, April, October, and November) and the dry season months are between December and February. From the daily records of data collected, the values of pressure (P) in hPa, temperature (T) in °C and relative humidity (H) in % were extracted, from which radio refractivity gradients were computed and then subjected to nonlinear time series analysis. The geographical and climatic characteristics of the five selected locations across the country are as shown in Fig. 1. The application of both LE and TE in this work reveals the anomalies or trends emerging from the internal dynamics of the RRG in the troposphere. Eqn. (11) and (12) can be used to compute for the Largest LE, where a positive LE represents evidence of chaos.

4. Results and discussion

In complex data analysis, the physical appearance of a dynamical ensemble can be represented by a nonlinear time series. The series may not actually reflect the internal activities of the dynamics which implies that it may not reveal the whole process going on in the system. In this section, the time series trend of the RRG for the five stations was categorized into the specified seasons. A system can possess either a periodic waveform (i.e. equal peaks), quasi-periodic waveform, chaotic waveform or hyperchaotic waveform depending on their initial conditions which is a function of the changes in meteorological parameters at time t. Fig. 2 shows the typical time series with different peaks for the five selected stations, which reflect the information of dynamical systems. However, Fig. 3 reveals the PPR of the RRG for the selected month of each specified season i.e. the rainy (concentrated data at the center), dry (random-like and concentrated at the center) and transition seasons. Internal dynamics of natural systems such as a hurricane, typhoon among others in nature are considered as hyperchaotic systems, that is, dynamic (unpredictable) ensemble. This is as a result of the movement of different micro-ensemble, assemble to form macro-ensemble such as the troposphere. The expectation of the dynamic state will be complex and not in any way reliable for the prediction of radio path in the area of communication.

It was observed that during the rainy season, RRG increases as a result of the concentrated point at the center of the phase space diagram (see Fig. 3a), while random-like behavior and center-like concentration was also noticed for the dry season (see Fig. 3b). Fig. 3c also reveals PPR for the transition periods.

Also, the choice of the delay time $\tau \leq 12$ and embedded dimension $m \geq 7$ for FNN drops below the value $\frac{1}{e}$ i.e. the lowest value of τ, is considered to be true for 2011 and 2012 data (see Fig. 4a and b). The embedding dimension is chosen from a system with a higher dimension and also from the distribution of time-delayed mutual information, a single value that seems to be good characterization across all the stations was picked following the Wallot concept [39].

Fig. 4c reveals the typical AMI for the RRG data, while Fig. 5 shows the positive LE across the selected locations from 2011 to 2012. Likewise, during the rainy season months, the RRG increases as a result of the suppression of chaoticity in the troposphere. That is the poor quality of radio signal equivalent to the positive value of LE or divergence of trajectory or expansion of volume along another direction.

It can also be observed clearly that the positive LE were generated from the five stations (see Fig. 5), where we observed lower LE during the rainy season and higher LE during the dry season months. Jos and Minna have their lowest LEs in the month of August and November, respectively. They also experience their highest LEs in February and March, respectively. Similarly, during the transition period (i.e. March-April and October-November), there is a sudden drop and sudden rise in LEs which indicate the onset or offset of rainy-harmattan periods. TE computed from Eqn. (13) also shows the same nonlinear trends for the five locations with regions of lower complexity especially during the rainy season months and higher complexity during the dry season months as depicted in Fig. 6.

For further evidence, RP was computed from Eqn. (17) which quantifies the complexity of the RRG for 2011 and 2012 (see Fig. 7). The process is deterministic with a short line segment that depicts positive maximum LE. However, parallel diagonal lines and short diagonal lines as observed in the selected rainy months (see Fig. 7a) and dry months (see Fig. 7(b)) are an indication of chaos. The transition to rainy and dry seasons period also occurs in Fig. 7(c) and Fig. 7(d) respectively, where some states were far from the normal chaotic behavior as a result of the influence of meteorological parameters during the onset and offset periods. The complexity of RRG in the troposphere is a major problem that can affect path clearance of the radio signals as well as causing propagation effects such as sub-refraction, super-refraction, or ducting.

In general, it is well known that during the rainy season, an increase in RRG is an indication of the higher complexity of the troposphere. For example, in the tropical region like Nigeria, the seasonal difference in RRG is mainly attributed to temperature or humidity inversion at 100 m height, while reflection in solar radiation and surface temperature might be responsible for the ground level (0 m). Other meteorological conditions such as high evaporation and passing of the cold air over the warm surface can equally responsible for the anomalies experienced in the radio-link propagation. However, the result is a short time prediction as the condition may change if there are any deformity and various hazardous events.

5. Conclusion

In this paper, the comparative study on the complexity of radio refractivity gradient using Chaotic Quantifiers have been studied for the 2011 and 2012 seasons. The short term prediction of disorderliness during the rainy, dry and transition months for the two years were observed and recorded. The aforementioned results reveal evidence of chaos with a higher refractivity gradient across the specified locations. Higher RRG signifies higher chaoticity which was observed during the rainy season compared to the dry season and transition periods for the five selected locations. The behavior of LE is actually directly proportional to the TS which confirms the high degree of complexity during the rainy season for the two years. In addition, the parallel and short lines noticed in RP also indicate the evidence of chaos. Also recorded surprisingly were the changes that occur during on-set and off-set transition periods due to seasonal rain-harmattan transition phase and dust-laden north-eastern wind. It is worthwhile necessary to investigate the effect of meteorological parameters and the hydrometeors on the troposphere in other to avoid fading of radio signals along with the radio communication links.
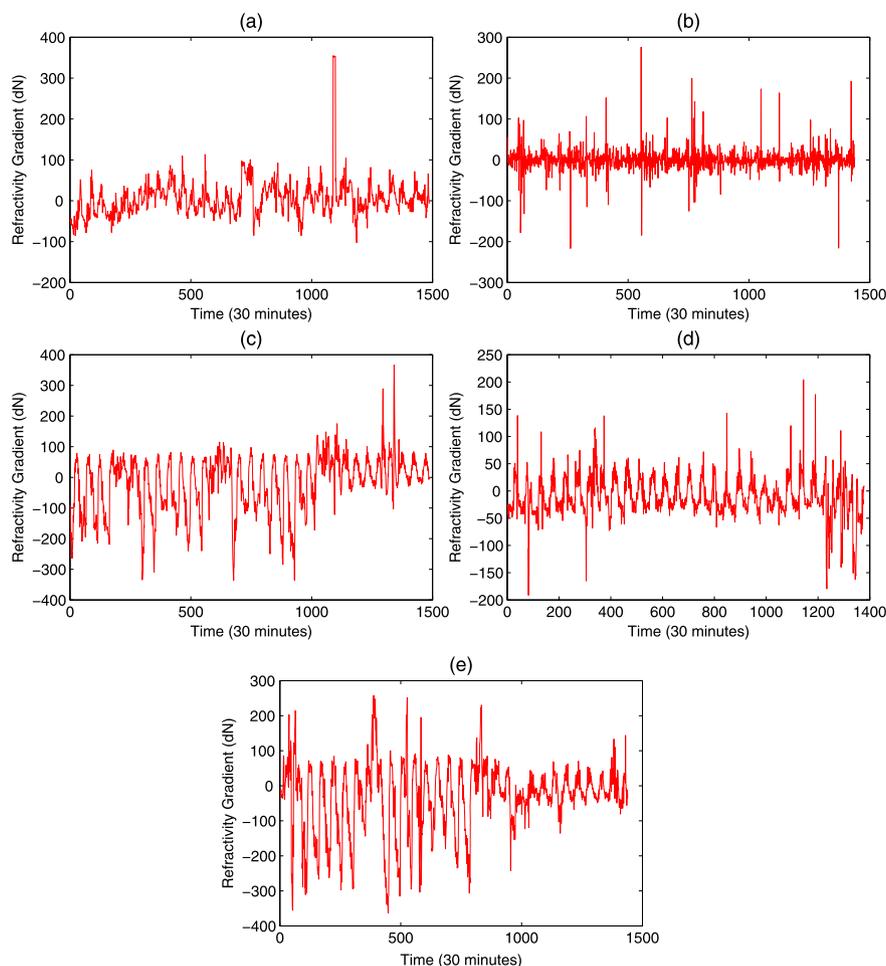
Fig. 2. Typical time series plots for the RRG for all the stations between January 1, 2011-30 December, 2012 in Nigeria: (a) Akure, (b) Enugu, (c) Jos, (d) Minna and (e) Sokoto.

Declarations

Author contribution statement

J.S. Ojo: Conceived and designed the experiments. A.O. Adelakun: Performed the experiments; Wrote the paper. O.V. Edward: Analyzed and interpreted the data; Contributed reagents, materials, analysis tools or data.

Competing interest statement

The authors declare no conflict of interest.

Additional information

No additional information is available for this paper.

References

[1] O.F. Dairo, L.B. Kolawole, Statistical analysis of radio refractivity gradient of the rainy-harmattan transition phase of the lowest 100 m over Lagos, Nigeria, J. Atmos. Sol.-Terr. Phys. (2017).

[2] S. Zheng, F. Han-Xian, Monitoring of ducting by using a ground-based gps receiver, Chin. Phys. B 22 (2) (2013) 1–5.

[3] S. Gadgil, The indian monsoon and its variability, Annu. Rev. Earth Planet. Sci. 3 (2003) 429–467.

[4] S. Leroyer, S.B. eLair, S.Z. Husain, J. Mailhot, Subkilometer numerical weather prediction in an urban coastal area: a case study over the vancouver metropolitan area, J. Appl. Meteorol. Climatol. 56 (6) (2014) 1433–1453.

[5] D. Sikka, S. Gadgil, On the maximum cloud zone and the itcz over indian longitudes during the southwest monsoon, Mon. Weather Rev. 108 (2003) 1840–1853.

[6] D. Sikka, S. Gadgil, Large-scale rainfall over india during the summer monsoon and its relation to the lower and upper tropospheric vorticity, Indian J. Meteorol. Hydrol. Geophys. 29 (1980) 219–231.

[7] B.R. Bean, E.J. Dutton, Radio Meteorology, Dover Publication Co., New York, 1968.

[8] A.T. Adediji, S.T. Ogunjo, Variations in non-linearity in vertical distribution of microwave radio refractivity, Prog. Electromagn. Res. M 36 (2014) 177–183.

[9] B.O. Ogunsua, J.S. Ojo, A.T. Adediji, Atmospheric chaoticity and complexity from radio refractivity derived from Akure station, Adv. Space Res. 6 (7) (2018) 1690–1701.

[10] R.J. Cornforth, West african monsoon 2012, Weather 68 (10) (2013) 256–263.

[11] S. Janicot, J.P. Lafore, C.D. Thorncroft, The west african monsoon, in: C.-P. Chang, Y. Ding, G.N.-C. Lau, R.H. Johnson, B. Wang, T. Yasunari (Eds.), The Global Monsoon System: Research and Forecast, 2nd edition, in: World Scientific Series on Asia-Pacific Weather and Climate, vol. 5, World Scientific Series, Singapore, 2011.

[12] C. Ramage, Monsoon Meteorology, vol. 15, Academic Press, San Diego, Calif, 1971.

[13] P. Webster, Monsoons, in: The Elementary Monsoon, John Wiley & Sons, 1987, pp. 3–32.

[14] H. Hsu, M. Lee, Topographic effects on the eastward propagation and initiation of the madden-julian oscillation, J. Climate 18 (2005) 795–809.

[15] S.L. Lavender, A.J. Matthews, Response of the West African monsoon to the madden-julian oscillation, J. Climate 22 (2009) 4097–4116.

[16] J.M. Aparicio, S. Laroche, An evaluation of the expression of the atmospheric refractivity for GPS signals, J. Geophys. Res. 116 (2011) 1–14.

[17] R.L. Freeman, Radio System Design for Telecommunications, John Wiley and SonsInc Pb, Hoboken, New Jersey, 2007, pp. 880.

[18] A.T. Adediji, M.O. Ajewole, Vertical profile of radio refractivity gradient in Akure South-West Nigeria, Prog. Electromagn. Res. C 4 (2008) 157–168.
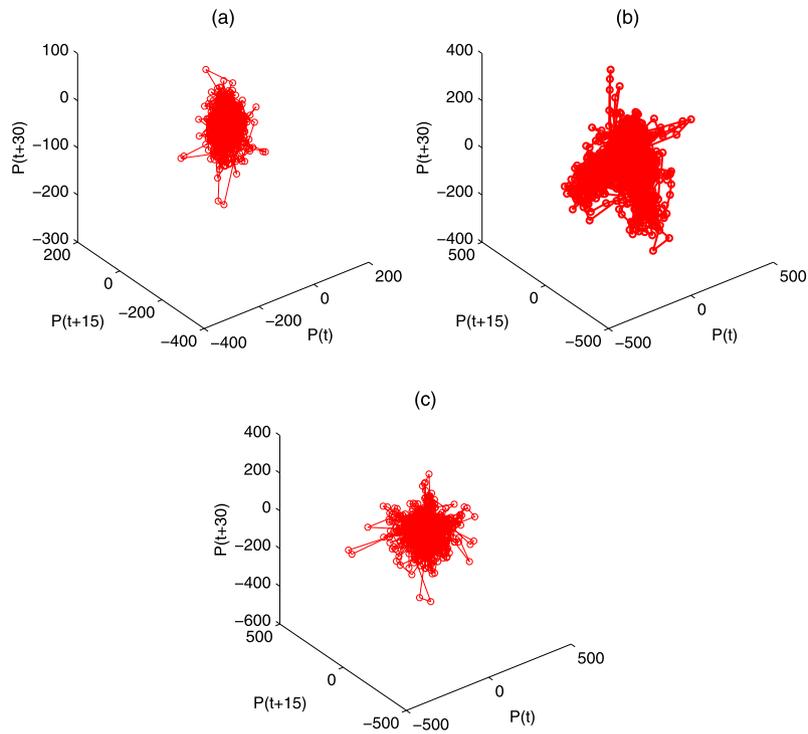
Fig. 3. Typical phase plot reconstructions for the radio refractivity gradient for selected locations during the (a) rainy season, (b) dry season and (c) transition season.
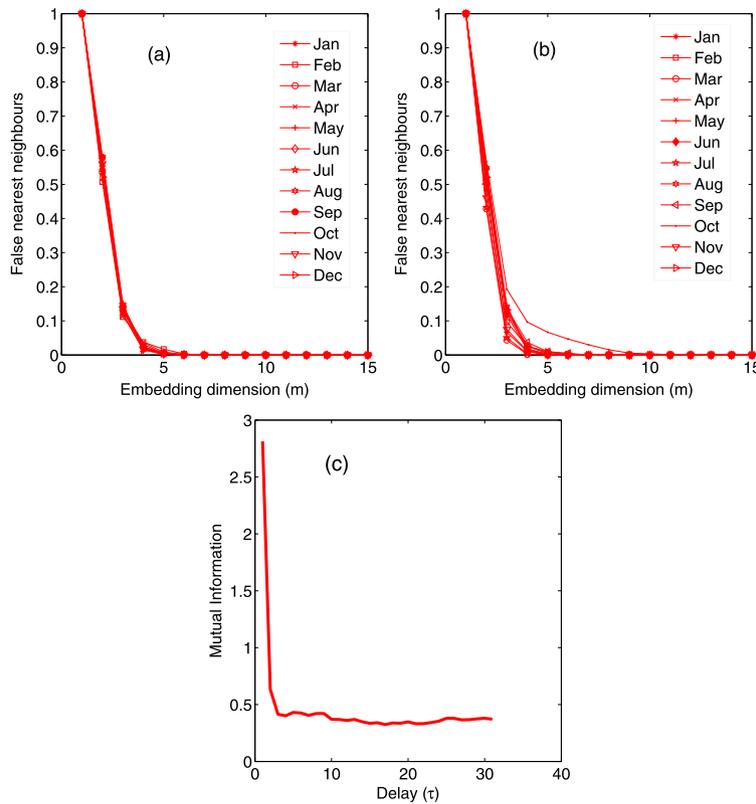

Fig. 4. Typical plot of false nearest neighbor against the embedding dimension of radio refractivity gradient for the selected locations for (a) 2011 and (b) 2012 season and (c) Average mutual information for RRG.

[19] B.O. Ogunsua, J.A. Laoye, I.A. Fuwape, A.B. Rabiu, The comparative study of chaoticity and dynamical complexcity of the low-latitude ionosphere over Nige-ria, during the quite and disturbed days, Nonlinear Process. Geophys. 21 (2014) 127–142.
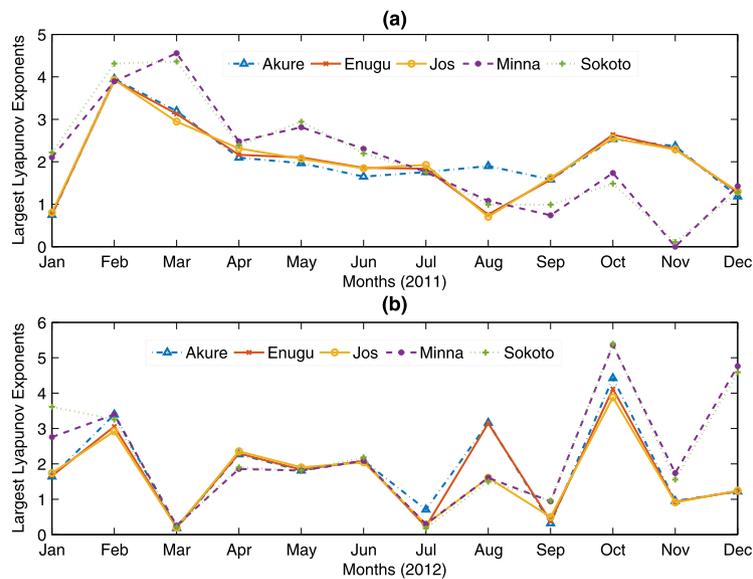
Fig. 5. Largest Lyapunov exponents for the radio refractivity gradient for the five locations for year (a) 2011 and (b) 2012.
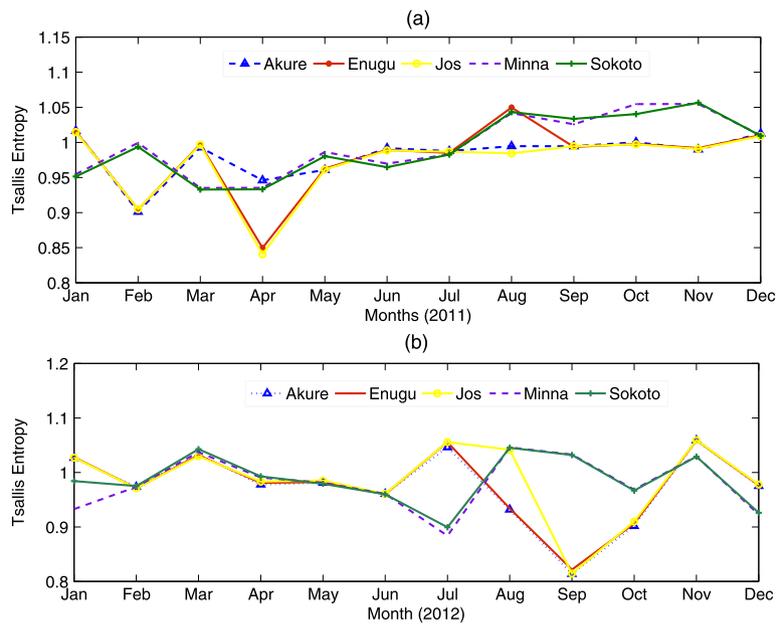

Fig. 6. Tsallis Entropy for the radio refractivity gradient for rainy, dry and transition periods for year (a) 2011 and (b) 2012.

[20] A.M. Fraser, H.L. Swinney, Independent coordinates for strange attractors from mutual information, Phys. Rev. A 33 (1986) 1134–1141.

[21] H.D.I. Abarbanel, R. Brown, J.J. Sidorowich, L.Sh. Tsimring, The analysis of observed chaotic data in physical systems, Rev. Mod. Phys. 65 (1993) 1331–1392.

[22] M.B. Kennel, R. Brown, H.D.I. Abarbanel, Determining minimum embedding dimension using a geometrical construction, Phys. Rev. A 45 (1992) 3403–3411.

[23] A. Wolf, J.B. Swift, J.A. Vastan, Determining Lyapunov exponents from a time series, Physica D 16 (1985) 285–317.

[24] C. Tsallis, Possible generalization of Boltzmann-Gibbs statistics, J. Stat. Phys. 52 (1988) 487–497.

[25] C. Tsallis, Generalized entropy-based criterion for consistent testing, Phys. Rev. E 58 (1998) 1442–1445.

[26] C. Tsallis, Nonextensive statistics: theoretical, experimental and computational evidences and connections, Braz. J. Phys. 29 (1999) 1–35.

[27] H. Kantz, T. Schreiber, Nonlinear Time Series Analysis, Cambridge University Press, 2003.

[28] J. Boon, C. Tsallis, Nonextensive Statistical Mechanics: New Trends, New Perspectives, Cambridge University Press, 2003.

[29] G. Balasis, I.A. Daglis, C. Papadimitrou, M. Kalimeri, A. Anastasiadis, K. Eftaxias, Dynamical complexity in D_{st} time series using non-extensive Tsallis entropy, Geophys. Res. Lett. 35 (2008) L14102.

[30] G. Balasis, I.A. Daglis, C. Papadimitrou, M. Kalimeri, A. Anastasiadis, K. Eftaxias, Investigating dynamical complexity in the magnetosphere using various entropy, Geophys. Res. Lett. 114 (2009) A00D06.

[31] A. Anastasiadis, L. Costa, C. Gonzales, C. Honey, M. Szeliga, D. Terhesiu, Measures of structural complexity in networks, in: Complex Systems Summer School 2005, Santa Fe, 2005.

[32] M. Baranger, V. Latora, A. Rapisarda, Time evolution of thermodynamic entropy for conservative and disipative chaotic maps, Chaos Solitons Fractals 12 (2002) 471–478.

[33] N. Kalogeropoulos, Weak chaos from Tsallis entropy, Qscience Connect 12 (2012).

[34] N. Kalogeropoulos, Varnishing largest Lyapounov exponent and Tsallis entropy, Qscience Connect 26 (2013).

[35] M. Coraddu, M. Lissia, R. Tonelli, Statistical descrptions of nonlinear systems at the onset of chaos, arXiv:condmat/0511736v1, Physica A 365 (2006) 252–257.

[36] J.P. Eckmann, S.O. Kamphorst, D. Ruelle, Recurrence plots of dynamical systems, Europhys. Lett. 5 (1987) 973–977.
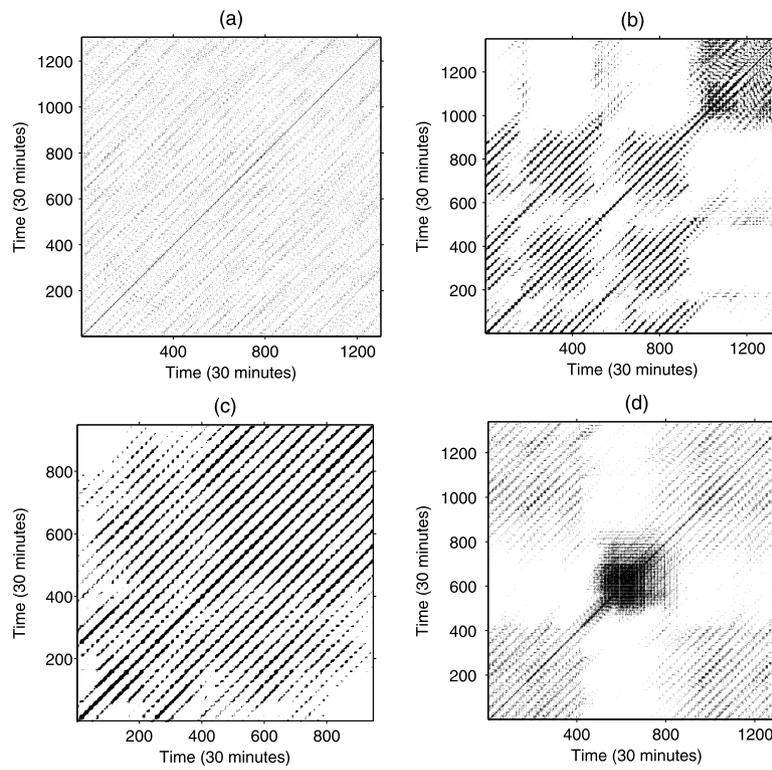
Fig. 7. Radio refractivity gradient recurrence plots for selected months during (a) rainy season, (b) dry season, (c) Transition to wet season period (March-April) and (d) Transition to dry season period (October-November).

[37] N. Marwan, Encounters with Neighbors: Current Development of Concepts Based on Recurrence Plots and Their Applications, PhD thesis, University of Potsdam, 2003, pp. 18–21.

[38] M. Thiel, M.C. Romano, J. Kurths, R. Meucci, E. Allaria, F.T. Arecchi, Influence of observational noise on the recurrence quantification analysis, Physica D 171 (2002) 138–152.

[39] S. Wallot, Multidimensional cross-recurrence quantification analysis (MdCRQA) - a method for quantifying correlation between multivariate time series, Multivar. Behav. Res. (2018).